Progress In Electromagnetics Research Letters, Vol. 108, 49–57, 2023

A Conformal Multi-Band MIMO Antenna for Vehicular Communications

Vanka Saritha[1, *] and Chakali Chandrasekhar[2]

Abstract—This paper proposes a conformal multiple band four port MIMO antenna for next generation vehicular communications in the extended UWB. The single element consists of a monopole antenna resembling a U-shaped structure with two branches folded and complimentary to each other. It uses coplanar waveguide feeding with a defected ground structure. The antenna is printed on a Kapton Polyamide flexible substrate having a thickness of 0.25 mm. The antenna has dimensions of $0.8\lambda \times 0.8\lambda \times 0.001\lambda$. It resonates at 2.6 GHz, 3.9 GHz, and 5.6 GHz which are used in vehicular communications, and can be used in sub-6 GHz 5G applications. It also provides band notches at 2.1 GHz, 3.5 GHz, and 4.5 GHz which enables it to mitigate the interferences from any narrow band devices operating in that range. All MIMO parameters are simulated and compared with the measured results, and are found to be in good agreement. The designed antenna can be mounted at any position of the vehicle as it has a conformal structure.

1. INTRODUCTION

Vehicular communication is an emerging space of communications between vehicles together with roadside infrastructure. Developments in wireless communications are creating potential distribution of information over real time communication between the vehicles and corresponding infrastructure. This has directed to solicitations to enhance the safety of vehicles and the communication between travelers and the Internet. Regularization exertions on vehicular communication are also ongoing to make vehicular conveyance harmless, greener, and at ease. Vehicles will be able to make use of cellular networks to converse with the Vehicle to Everything (V2X) management system in vehicle to network (V2N) communication. V2N operates with the dedicated short-range communications (DSRC) standard for communicating with other vehicles and also with the infrastructure present on the roads. This extent of connections permits a vehicle to be treated as a "device", exactly like smart mobiles and wearable devices. Retrieving mobile-network operators' LTE, infrastructure and DSRC systems permit vehicles to obtain broadcast alerts concerning the status of road conditions like accidents, congestion, weather, etc., which are identified as vehicle to infrastructure (V2I) communications. Communication through neighboring vehicles by means of the mobile network and DSRC is identified as vehicle to vehicle (V2V) communication. Connected and independent vehicles (CAVs) combine a variety of diverse technologies with an intention of moving people and goods and chattels on roads with added safety and dexterously. Multiple-input multiple-output (MIMO) systems have grown in responsiveness in latest research due to their competence to operate multi-antennas concurrently and due to the rise in channel capacity without any added spectrum or transmitted power necessities. MIMO designs allow the provision of effective and consistent communications with the benefits of higher data rates and multi-Gbps data.

Received 5 September 2022, Accepted 7 December 2022, Scheduled 13 December 2022
* Corresponding author: Vanka Saritha (vankasaritha20@gmail.com).
[1] Research Scholar, Department of ECE, Jawaharlal Nehru Technological University, Anantapur, Ananthapuramu, Andhra Pradesh, India. [2] Professor, Department of ECE, Sri Venkateswara College of Engineering, Tirupati, Andhra Pradesh, India, Affiliated to Jawaharlal Nehru Technological University, Anantapur, Ananthapuramu.

CAVs, attached with intelligent road structure, will outbreak certain severe environmental, social, and profitable disputes which will become worse if no action is engaged. Designing an antenna for vehicular applications is indeed a challenging task for RF engineers. A new fractal microstrip patch antenna on RT duroid PCB laminated material is presented in [1] with DSRC ranging from 5.850 to 5.925 GHz service band. An automotive antenna for 5G and Vehicle to Everything (V2X) communications operating in multiple bands is proposed in [2]. It is designed to fit the regularly used shark fin radome. A compact, highly directive single-band 2×2 and 4×4 antenna arrays for 5.8 GHz and also for 28 GHz intended for UAV applications to install UAV by means of a 5G network is presented in [3]. This provides a wider bandwidth at both operating frequencies.

An antenna module for automotive 5G communications is designed in [4] to cover the frequency band from 24.25 to 27.5 GHz. It consists of 8 dual polarized stacked patches. An Electronic Band Gap (EBG) structure is employed in order to reduce the radiation pattern distortion due to surface wave propagation. A compact CPW-fed MIMO antenna for upcoming generation vehicular transportation is proposed in [5]. It operates at 3.5 GHz used for the LTE band and also at 5.9 GHz used for DSRC band. It is suitable for the deployment of V2V, V2I, and V2N setups. A UWB antenna designed to work for small power that uses IoT or WLAN mode (2.1 GHz–3.9 GHz) and WLAN or DSRC mode (5–6.5 GHz) has been extended to make a four-port MIMO antenna which is vertically polarized for the improvement of link consistency [6]. An investigation for channel model is done, and a confocal stochastic geometry ellipsoid model for modeling the MIMO channels to achieve lower correlation is developed in [7]. A 3D UWB MIMO antenna with eight ports is presented in [8] with two band notches for vehicular communications based on polarization diversity scheme with Substrate Integrated Waveguide (SIW). The SIW established is combined with an L-shaped slot stub which is parasitic, a radiator to provide the notch of WLAN, and also an L-shaped stub coupled at the ground plane to provide the notch at the X-band. A novel compact MIMO antenna providing a wider impedance bandwidth and sufficient port separation for a vehicular base station is suggested in [9]. In this design, there are four identical monopole-based antenna elements that are vertically-polarized, symmetrical around the central axis, and positioned 90 degrees away from each element. It operates from 1.95 GHz to 6.25 GHz. A novel DRA MIMO antenna with polarization diversity which operates from 2.5 GHz to 3 GHz is presented in [10]. In [11], a MIMO antenna consisting of a two element antenna resembling a T-shape using partial ground structure and a split ring resonator for 5G-based vehicular communications is printed on an RT duroid 5880 substrate. It provides 6.3 and 3.96 GHz bandwidths operating in the ranges of 26.83–33.13 GHz and 34.17–38.13 GHz. It is located on a vehicle in a virtual environment by means of the ANSYS SAVANT tool. Various MIMO antennas with various ports are discussed in [12]. In [13], a MIMO antenna with four elements arranged in an orthogonal fashion provides sufficient isolation. A multiband fractal antenna for IoT applications is presented in [14]. A novel slotted planar antenna with a "回" structure operating at multiple bands (1.58–1.77 GHz, 2.1–2.50 GHz, 3.61–4.09 GHz, and 4.75–6.5 GHz) suitable for navigation applications is proposed in [15]. An antenna of HUI pattern shaped radiator is proposed in [16] covering 1.49 to 1.60 GHz, 1.87 to 2.51 GHz, and 4.63 to 5.34 GHz bands for navigational purposes. This paper proposes the design and analysis of a compact printed MIMO antenna for vehicular communications.

2. DESIGN AND EVOLUTION OF THE CONFORMAL ANTENNA

The radiating part of the antenna is made as a copper layer and is pasted onto the Kapton Polyamide substrate which has a relative permittivity of 3.55. It has a thickness of 0.25 mm and a loss factor of 0.02. The required simulations are carried out using HFSS software. The dimensional values of the proposed structure are as specified in Table 1.

The antenna structure is portrayed in Fig. 1(a). Its development to obtain desired resonant bands for vehicular applications at 2.6 GHz, 3.9 GHz, and 5.6 GHz correspondingly is depicted in Fig. 2. The orientation of the antenna is shown in Fig. 1(b).

2.1. Development of Multi Band Characteristics

Stage-1: Consists of a monopole antenna made up of symmetrical folded branches. The structure of the ground is a defected rectangular structure. This structure provides resonance at 3.1 GHz.

Stage-2: Includes, in addition to stage-1, a second iteration of folding done as shown in Fig. 2. This provides an additional resonance at 3.8 GHz.

Stage-3: In addition to stage-2, the defected ground plane is modified as shown in Fig. 2, and an additional resonance is observed at 7 GHz.

Stage-4: In addition to stage-3, another branch is folded complimentarily to the previous branch as shown in Fig. 2, and the feedline is optimized. This provides resonances at 2.0 GHz, 3.1 GHz, 4.0 GHz, and 5.8 GHz with a return loss of 8 dB.

Stage-5: In order to provide a better return loss, the feed line is further optimized, and the cavity between the ground plane and feedline is also adjusted. This provides resonances at 2.0 GHz, 2.6 GHz, 3.8 GHz, and 5.6 GHz which are suitable for vehicular communications. It also simultaneously provides band notches at 2.1 GHz, 3.5 GHz, and 4.5 GHz.

Table 1. Dimensions of the antenna.

Parameter	Value (mm)	Parameter	Value (mm)	Parameter	Value (mm)
$L1$	60	$L8$	4	$T1$	2
$L2$	20	$W1$	60	$T2$	1.2
$L3$	10	$W2$	25	$T3$	0.6
$L4$	30	$W3$	18	$T4$	1
$L5$	23	$W4$	18	$G1$	20
$L6$	15	$W5$	9	$G2$	2
$L7$	15	$W6$	6		

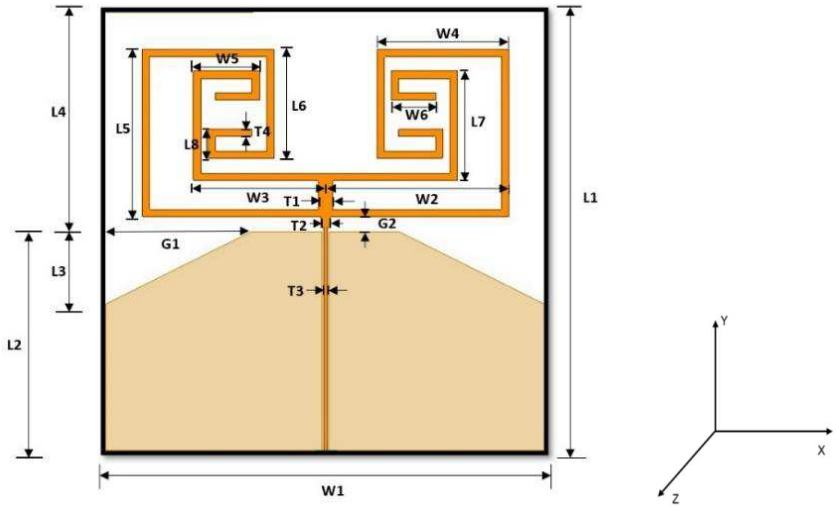

(a) Radiating patch (b) Axes

Figure 1. Antenna structure with all the dimensions.

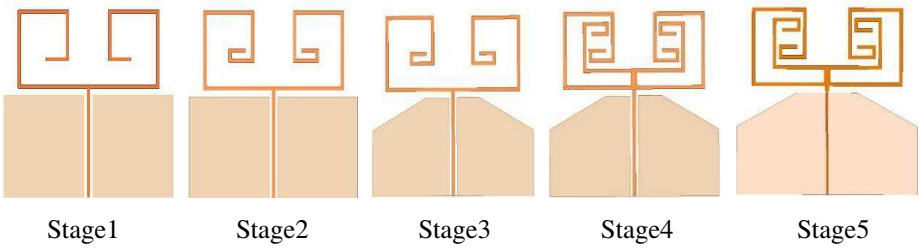

Figure 2. Evolution of proposed antenna for multiband characteristics at various stages.

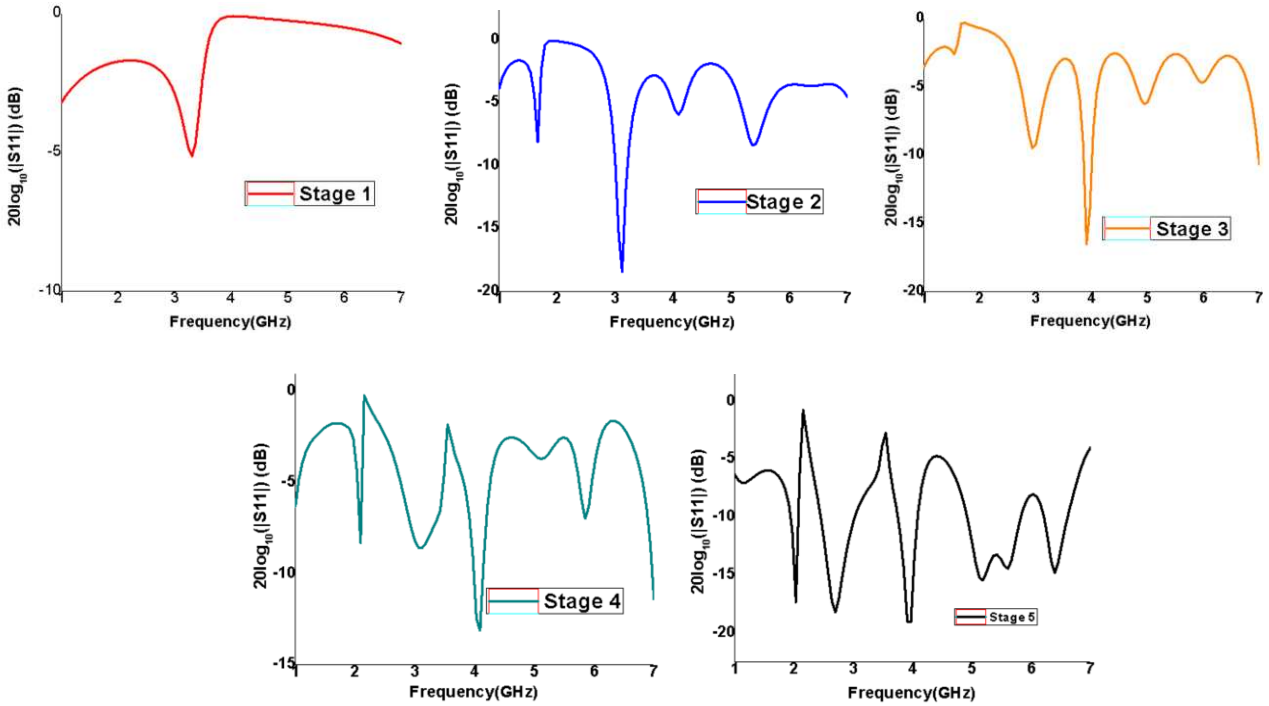

Figure 3. Reflection Coefficient (simulated) of the proposed antenna for various stages.

The reflection coefficients at various stages during the development of the proposed antenna are shown in Fig. 3.

3. QUAD PORT CONFORMAL MIMO ANTENNA

In the configuration of the MIMO antenna, in order to avoid mutual coupling, the arrangement of elements is orthogonal, and to improve compactness, suitable spacing is provided in between every two elements. The copper sheets of the proposed structure are pasted on to Kapton Polyamide. The measurements are done intending to certify the antenna capabilities aimed at real-world usage. A picture of the fabricated prototype is shown in Fig. 4. The analysis and comparison between the measured and simulated results are given below.

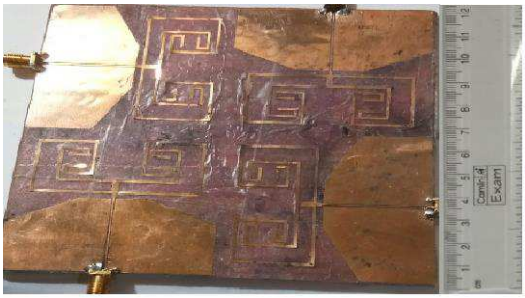

Figure 4. Fabricated model of the MIMO antenna.

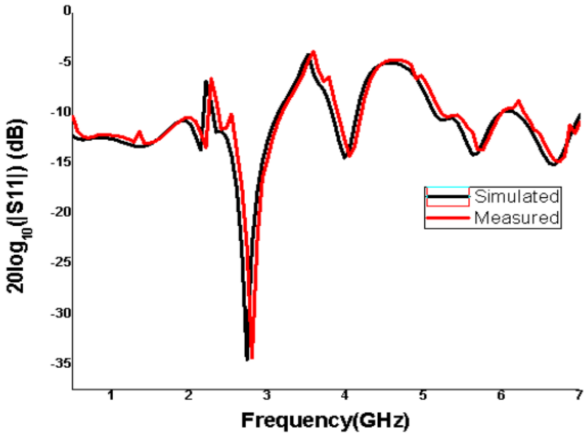

Figure 5. Simulated and measured reflection coefficient magnitude plots.

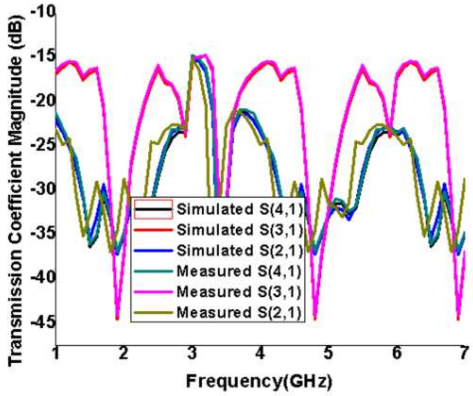

Figure 6. Simulated and measured transmission coefficient magnitude plots.

4. EXPERIMENTAL RESULTS

4.1. Scattering Parameters

A vector network analyzer is used to measure the scattering parameters of the fabricated model of the MIMO antenna. The measured as well as simulated reflection coefficients are shown in Fig. 5, and the curves of transmission coefficients for the antenna are given in Fig. 6. The operating range of proposed antenna is from 2 GHz to 6 GHz with three notches at 2.1 GHz, 3.5 GHz, and 4.5 GHz. The proposed antenna resonates at 2.6 GHz, 3.9 GHz, and 5.6 GHz. The isolation amongst the elements is depicted to be well below -15 dB all over the operational band and well below -22 dB at resonating frequencies.

The measured and simulated results are well correlated. However, due to the misalignment in pasting copper layer which leads to losses or due to usage of the coaxial cables for the duration of the measurement process, a trivial insignificant change is distinguished.

4.2. Radiation Patterns

Far field radiation patterns are shown in Fig. 7 while the antenna functions at the three operating frequencies of 2.6, 3.9, & 5.6 GHz. Fig. 7(a) demonstrates zenith-plane radiation patterns. Fig. 7(b) shows azimuthal-plane radiation patterns. The black color curve specifies simulated pattern as red colour curve specifies measured pattern.

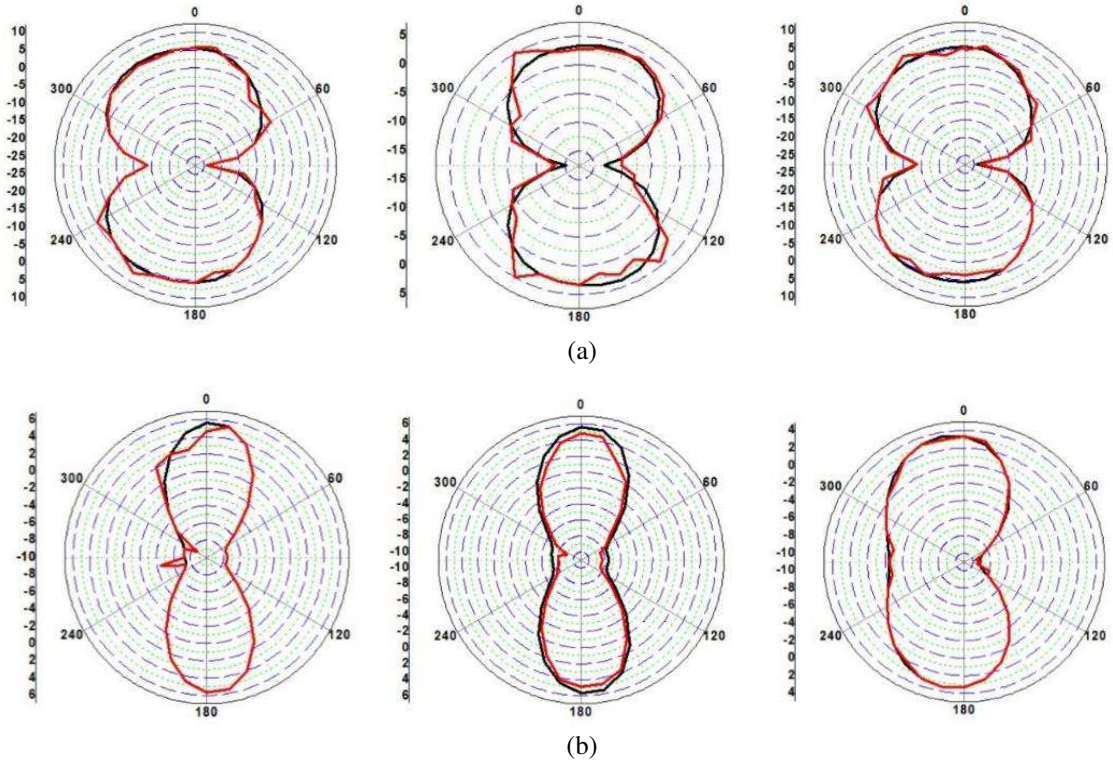

Figure 7. Radiation patterns in the (a) Zenith-plane (x-z plane), (b) azimuthal-plane (x-y plane) at the resonating frequencies 2.6 GHz, 3.9 GHz and 5.6 GHz.

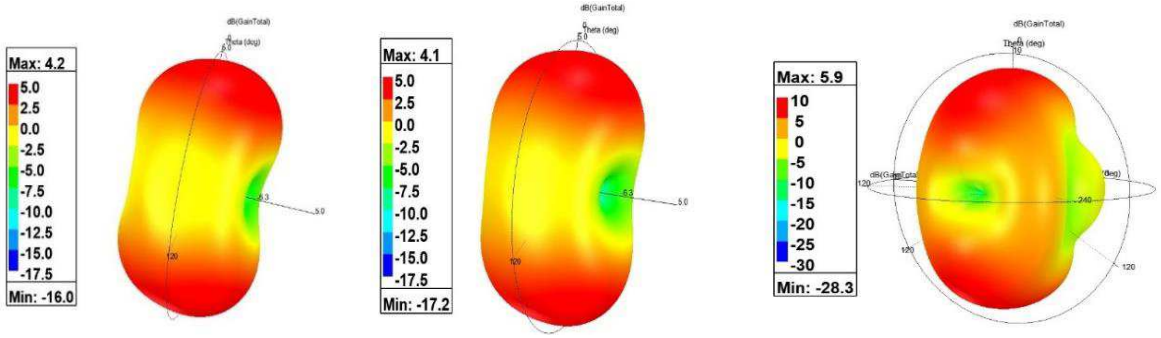

(a) 2.6 GHz (b) 3.9 GHz (c) 5.6 GHz

Figure 8. Three-dimensional radiation patterns at the resonating frequencies 2.6 GHz, 3.9 GHz and 5.6 GHz.

4.3. 3D Radiation Patterns

The 3D patterns at 2.6 GHz, 3.9 GHz, and 5.6 GHz are shown in Fig. 8.

The value of gain at 2.6 GHz, 3.9 GHz, and 5.6 GHz is observed to be 4.2 dBi, 4.1 dBi, and 5.9 dBi respectively.

5. PERFORMANCE PARAMETERS OF MIMO CONFIGURATION

The key performance indicators of any MIMO antenna are ECC, DG, as well as CL. They have been investigated for validation. The parameters are deliberated further as follows.

5.1. Envelope Correlation Coefficient (ECC)

ECC is a significant factor that insists in the diversity performance intended for each MIMO system. An ECC value of less than 0.1 represents flawless performance. It is evaluated by means of far field parameters and given by the following relation [13].

$$\rho_e = \frac{\left|\int_0^{2\pi}\int_0^{\pi}\left(XPR\cdot E_{\theta 1}\cdot E_{\theta 2}^{*}\cdot P_{\theta}+E_{\varphi 1}\cdot E_{\varphi 2}^{*}\cdot P_{\varphi}\right)d\Omega\right|^2}{\int_0^{2\pi}\int_0^{\pi}\left(XPR\cdot E_{\theta 1}\cdot E_{\theta 2}^{*}\cdot P_{\theta}+E_{\varphi 1}\cdot E_{\varphi 2}^{*}\cdot P\varphi\right)d\Omega X\int_0^{2\pi}\int_0^{\pi}\left(XPR\cdot E_{\theta 1}\cdot E_{\theta 2}^{*}\cdot P_{\theta}+E_{\varphi 1}\cdot E_{\varphi 2}^{*}\cdot P\varphi\right)d\Omega} \tag{1}$$

The ECC curves for simulated and measured ones are shown in Fig. 9. It is confirmed that values of ECC are well below 0.05 at the desired resonant frequencies.

5.2. Diversity Gain

Diversity gain represents transmission power loss while schemes of diversity that exist were implemented on the single component used for any MIMO configuration. This is calculated using Equation (2) given below. Fig. 10 shows that Dg remains close to 10 dB at all the desired resonant frequencies, which demonstrates a worthy diversity presentation.

$$Dg = 10\sqrt{1-E^2} \tag{2}$$

In the above Equation (2), E denotes the envelope correlation coefficient. It is plotted in Fig. 10.

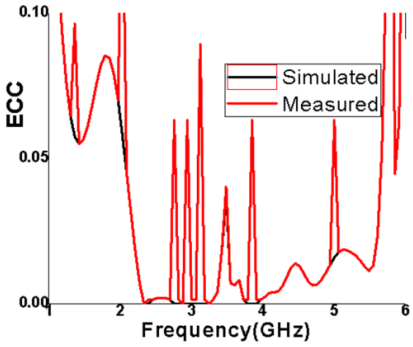

Figure 9. Simulated and measured plots of the envelope correlation coefficient.

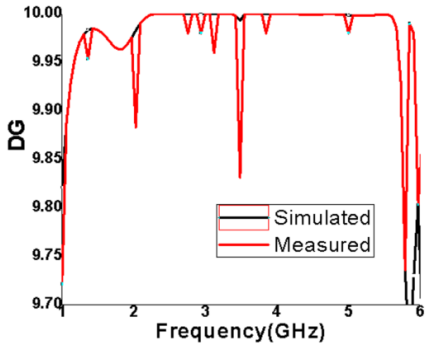

Figure 10. Simulated and measured plots of the diversity gain.

5.3. Channel Capacity Loss (CL)

The specifics of CL of any MIMO system is moreover a significant performance. It is estimated by below formulae (3), (4), & (5). Fig. 11 clarifies that the achieved CL is lower than the practical customary value of 0.2 bits/second/Hertz at the operating frequencies.

$$CL = -\log_2 \det(p) \tag{3}$$

where p is the correlation matrix specified by $p = \begin{bmatrix} \alpha_{11} & \alpha_{12} \\ \alpha_{21} & \alpha_{22} \end{bmatrix}$.

The elements of the matrix are articulated as follows

$$\alpha_{mm} = 1 - (|S_{mm}|^2 - |S_{mn}|^2) \tag{4}$$

$$\alpha_{mn} = -(S_{mm}^{*}S_{mn} + S_{nm}S_{nn}^{*}) \tag{5}$$

The group delay plots amongst any two ports are shown in Fig. 12. They vary between 0.80 and 2 ns except at the operated bands.

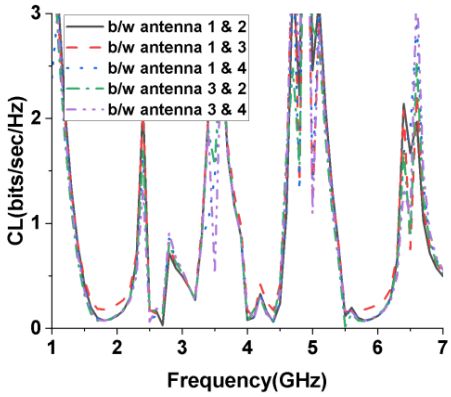

Figure 11. Plots of the Channel capacity loss.

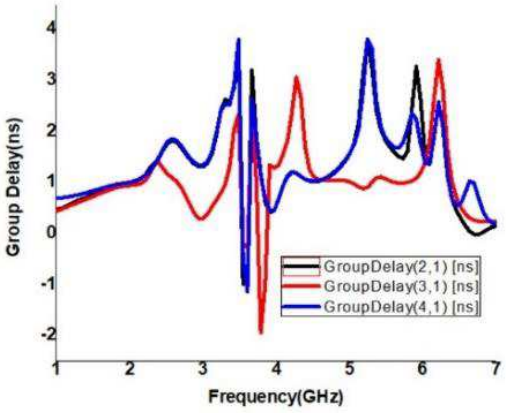

Figure 12. Plots of the group delay.

Table 2 displays the assessment of the performances of MIMO antennas resonating at different operating frequencies in cited references.

Table 2. Assessment of the performances of MIMO antennas in the literature.

Ref	Size of material in wavelength	Material	Operating band (GHz)	Isolation (dB)	ECC
[6]	$0.45\lambda * 0.3\lambda * 0.33\lambda$	FR4	4.1&10	> 15	< 0.5
[8]	$0.6\lambda * 0.6\lambda * 0.5\lambda$	FR4	4.5&12	> 20	< 0.002
[9]	$0.5\lambda * 0.5\lambda * 0.35\lambda$	FR4	3.5&5.5	> 16.5	< 0.028
[10]	$0.87\lambda * 0.87\lambda * 0.43\lambda$	FR4	2.6	> 20	< 0.5
[11]	$0.12\lambda * 0.25\lambda * 0.08\lambda$ (2 port)	Roger RT duriod 5880	26.8&37.8	$>= 10$	< 0.025
Proposed	$0.8\lambda * 0.8\lambda * 0.001\lambda$	Kapton Polyamide	2.6, 3.9&5.6	> 22	< 0.025

The above comparison shows that the proposed antenna is very compact in dimensions and conformal and has good isolation. There are no quad port conformal antennas operating at multibands for vehicular communications as per authors' knowledge with similar dimensions.

6. CONCLUSION

This paper focuses on compactness and conformality of a planar MIMO antenna to operate in multibands for vehicular communications. This proposed antenna resonates at three bands with impedance bandwidths 2.3 GHz–3.1 GHz, 3.8 GHz–4.1 GHz, and 5.1 GHz–5.8 GHz centered at 2.6 GHz, 3.9 GHz, and 5.6 GHz, respectively, and is suitable for sub-6 GHz 5G vehicular communications. Simultaneously, it also mitigates the interferences from any narrow band devices operating at 2.1 GHz, 3.5 GHz, and 4.5 GHz. The folding of the branches plays a major role to get resonances at the required lower frequencies.

REFERENCES

1. Kalyan, K. S. and C. Anirban, "Design of a right-handed circularly polarized printed antenna for vehicular communication," *Wireless Pers. Comm.*, Vol. 121, No. 4, 735–2756, 2021.

2. Riccardo, F. C., L. Stefano, M. Federico, et al., "3D automotive antenna for 5G and V2X communications," *2021 XXXIVth General Assembly and Scientific Symposium of the International Union of Radio Science*, 1–4, 2021.
3. Imran, A. Z. M., M. L. Hakim, A. Razu, et al., "Design of microstrip patch antenna to deploy unmanned aerial vehicle as UE in 5G wireless network," *Int. J. of Electrical. & Computer. Eng.*, Vol. 11, No. 5, 4202–4213, 2021.
4. Stefano, L., A. Mazzinghi, M. Cerretelli, et al., "Millimeter wave automotive antenna for 5G communications," *2021 XXXIVth General Assembly and Scient Symposium of the Int Union of Radio Science*, 2021.
5. Sujanthnarayan, K. G., J. A. Baskaradas, D. Rajeshkumar, et al., "Design of a CPW fed compact MIMO antenna for next generation vehicle to everything (V2X) communication," *Wireless Pers. Comm.*, Vol. 120, No. 3, 2021.
6. Bhakkiyalakshmi, R. and M. S. Vasanthi, "Novel four-port reconfigurable filtering MIMO antenna for multi-standard automotive communications," *AEU — Int. J. Electronics and Comm.*, Vol. 146, 154108, 2022.
7. Liu, F., "A stochastic confocal ellipsoid channel model for high speed railway MIMO communication systems," *Phy. Comm.*, Vol. 52, 101616.1–101616.6, 2022.
8. Prabhu, P. and S. Malarvizhi, "Design and packaging of polarization diversity 3D-UWB MIMO antenna with dual band notch characteristics for vehicular communication applications," *AEU — Int. J. Electronics and Comm.*, Vol. 138, No. 16, 153869, 2021.
9. Wang, W., Z. Zhao, Q. Sun, et al., "Compact quad-element vertically-polarized high-isolation wideband MIMO antenna for vehicular base station," *IEEE Trans. on Vehicular Tech.*, Vol. 69, No. 9, 10000–10008, 2020.
10. Ajay Kumar, D., S. Anand, S. Ashutoshkumar, et al., "Circularly polarized quad-port MIMO dielectric resonator antenna with beam tilting feature for vehicular communication," *IETE Tech. Review.*, Vol. 39, No. 2, 389–401, 2022.
11. Venkateswararao, M., B. T. P. Madhav, J. Krishna, et al., "CSRR-loaded T-shaped MIMO antenna for 5G cellular networks and vehicular communications," *Int. J. RF and Microwave Comput.-Aided. Eng.*, Vol. 29, No. 1, 14 pages, 2019.
12. Saritha, V. and C. Chandrasekhar, "A study and review on frequency band notch characteristics in reconfigurable MIMO-UWB antennas," *Wireless Pers. Comm.*, Vol. 118, No. 4, 2631–2661, 2021.
13. Saritha, V. and C. Chandrasekhar, "A compact wide band MIMO antenna with quadruple notches in UWB," *Progress In Electromagnetics Research M*, Vol. 108, 237–247, 2022.
14. Pravallika, I., S. Harsha, N. S. Manasa, et al., "Analysis and design of a low profile multiband antenna for IoT applications," *Int. J. Innovative Tech. and Exploring Eng.*, Vol. 8, No. 4, 535–539, 2019.
15. Yu, Z., Z. Lin, X. Ran, Y. Li, B. Liang, and X. Wang, "A novel "回" pane structure multiband microstrip antenna for 2G/3G/4G/5G/WLAN/navigation applications," *International Journal of Antennas and Propagation*, Vol. 2021, Article ID 5567417, 15 pages, 2021.
16. Xie, T., J. Yu, Y. Li, Z. Yu, and Z. Lin, "A novel "回" pattern branch antenna for 3G\4G\WLAN\bluetooth\navigation applications," *International Journal of Antennas and Propagation*, Vol. 2021, Article ID 1559519, 7 pages, 2021.